Pflügers Arch – Eur J Physiol (1999) 438:656–664
Digital Object Identifier (DOI) 10.1007/s004249900089

ORIGINAL ARTICLE

Yoshitaka Oku · Swen Hülsmann · Weiqi Zhang
Diethelm W. Richter

Modulation of glycinergic synaptic current kinetics by octanol in mouse hypoglossal motoneurons

Received: 16 November 1998 / Received after revision: 21 May 1999 / Accepted: 1 June 1999 / Published online: 20 July 1999

Abstract Octanol-induced changes in the kinetics of glycinergic inhibitory postsynaptic currents (IPSCs) were investigated by whole-cell recording from hypoglossal motoneurons in mouse brainstem slices. Octanol (1 mM) prolonged the decay time constants (τ_{decay}) of stimulus-evoked IPSCs (e-IPSCs) by 202±67% (SE). The depression of e-IPSC amplitudes was dose-dependent with an EC_{50} of 475 µM. Octanol also reduced the amplitude and prolonged the decay time constant of glycinergic currents evoked by local pressure ejection of glycine (I_{gly}). Replacement of extracellular Na^+ by choline and application of the specific glycine transporter GLYT1 inhibitor, sarcosine, lengthened τ_{decay} of I_{gly}, but did not change the decay time constants of e-IPSCs. Intracellular acidification by the weak organic acid salt sodium propionate (30 mM) reduced the e-IPSC amplitude by 22±9% and prolonged τ by 18±6%. Sodium propionate also prolonged the decay time constants of I_{gly} by 28±11%. The observed effects on decay kinetics were much smaller than those caused by octanol. The data show that octanol prolongs the decay time course of glycinergic synaptic currents by mechanisms independent of glycine uptake or intracellular acidification. We conclude that the effects were most probably due to direct action on postsynaptic glycine receptors.

Key words Gap junction blocker · Glycine uptake · Intracellular acidification · Synaptic transmission

Y. Oku · S. Hülsmann · W. Zhang · D.W. Richter
Department of Neurophysiology,
Centre of Physiology and Pathophysiology,
University of Göttingen, Humboldtallee 23,
D-37073 Göttingen, Germany

Y. Oku (✉)
Department of Medical Systems Control,
Institute for Frontier Medical Sciences, Kyoto University,
53 Kawahara-cho, Shogoin, Sakyo-ku, Kyoto 606–8397 Japan
e-mail: oku@ frontier.kyoto-u.ac.jp
Tel: +81-75-7513880
Fax: +81-75-7514647

Introduction

In neonatal animals, gap junctional coupling has been described to occur between neuroblasts of the ventricular zone [23], neocortical neurons [10, 29, 33], as well as putative motoneurons in the brainstem [31]. The degree of this intercellular coupling decreases to a great extent as the animals mature [10, 29, 33]. Although the functional role of intercellular coupling in neonatal animals is not well understood, it might serve to synchronize electrical and biochemical behavior among functionally related neurons. It has been proposed that in the ferret visual cortex gap junctions are a temporary communicating system that is replaced by chemical synapses during maturation [20]. Gap junction blockers have been used frequently to distinguish between mechanisms mediated through intercellular coupling by gap junctions and those mediated through synaptic transmission (e.g. [27]). For this purpose, we considered it important to have information that describes the effects of a well-known gap junction blocker, octanol, on chemical synaptic transmission.

Octanol, a long-chain alcohol, is a well-characterized agent that reduces gap junction conductance [9, 19, 33]. However, the underlying mechanisms remain obscure. Octanol application to cultured rat hippocampal astrocytes causes an initial intracellular acidification of the cytosol, which is followed by a persistent alkalization in most cells [28]. Since intracellular acidification uncouples gap junctional connections between neurons in embryonic rat cortex [23, 25], the uncoupling action of octanol may be attributable partly to the initial acidification of the cytosol. However, it has been shown that octanol also uncouples hepatocytes without changing intracellular pH [28].

The effects of octanol on ligand-gated ion channels have been studied extensively using molecular cloning techniques [12, 16]. It has been found that octanol potentiates the function of homomeric glycine [24] and type-A γ-aminobutyric acid ($GABA_A$) [12] receptors expressed in *Xenopus* oocytes. The potentiation of glycine receptor

function by octanol is comparable to ethanol-induced enhancement of glycinergic currents in cultured spinal neurons of mice [1, 2].

Glycine is a well-established inhibitory neurotransmitter in the spinal cord and brainstem of vertebrates [11]. Glycinergic synaptic transmission can be influenced by octanol through various factors in addition to its direct action on glycinergic receptors. Firstly, octanol may affect the removal of glycine from the synaptic cleft by interfering with uptake and diffusion, through its action on glial gap junctions. Secondly, octanol may influence presynaptic neuronal activity by reducing low-threshold calcium conductance [22, 34]. Thirdly, octanol may act on glycinergic receptors indirectly by changing intracellular pH. Fourthly, octanol may change the electrotonic properties of neurons by uncoupling gap junctions, especially in neonatal animals. In order to evaluate and differentiate between these mechanisms, we investigated the effects of octanol, glycine uptake, and intracellular acidification on stimulus-evoked synaptic currents and glycine-induced currents in mouse hypoglossal motoneurons.

Materials and methods

Preparation

Experiments were performed on neonatal NMRI mice (1–6 days old) of either sex. Animals were anesthetized with diethylether, and rapidly decapitated. The brainstem was removed and placed in carbogen-bubbled (95% O_2 – 5% CO_2) ice-cold artificial cerebrospinal fluid (ACSF; see below for composition). Transverse slices (thickness 200 µm) were cut at the level of area postrema with a vibratome (Campden Instruments, London, UK). Slices were stored in ACSF at room temperature (20–23°C) for at least 1 h before measurements.

Recording

Slices were kept submerged by means of a platinum grid with nylon meshes for mechanical stabilization. The chamber was mounted on a fixed-stage microscope (Zeiss Axioscope, Germany) and continuously perfused with ACSF (room temperature; 20–23°C) at a flow rate of 2–4 ml/min. The volume of the chamber and circulation lines was less than 2 ml. Hypoglossal motoneurons were identified visually with Nomarski optics by their location, size, and shape. We used neonatal animals because patching hypoglossal motoneurons becomes difficult as the animal matures, probably due to the arborization of the dendritic tree [6]. Whole-cell recordings were obtained with a discontinuous single-electrode current- and voltage-clamp amplifier (NPI SEC-05L; Tamm, Germany) at a switching frequency of 30–40 kHz (duty cycle: 25%). The series resistance compensation was not performed, because recordings with discontinuous VC-amplifiers such as SEC-5 are nominally independent of series resistance [13]. Patch electrodes were pulled from borosilicate glass capillaries (Clark Electromedical, Pangbourne, UK) on a programmable pipette-puller (Sutter Instruments P-87; USA) and had a tip diameter of about 2 µm. Filled with electrode solution, they had a resistance of 2–5 MΩ. Currents were filtered at 1.3 kHz with a four-pole Bessel filter and digitized at 10 kHz using an interface (ITC-16; HEKA, Lambrecht, Germany) and "Pulse" software (v.8.10; HEKA, Lambrecht, Germany). Leak currents were subtracted on-line by means of an alternating leak average protocol during the recording of stimulus-evoked inhibitory postsynaptic currents (e-IPSC). Data were stored on a hard disk for off-line analysis.

Solutions

The ACSF contained (in mM): 118 NaCl, 3 KCl, 1.5 $CaCl_2$, 1 $MgCl_2$, 1 NaH_2PO_4, 25 $NaHCO_3$, and 30 D-glucose. The osmolarity of the ACSF was 310 mosmol/l, and pH was adjusted to 7.4 by NaOH. During e-IPSC recordings, 2.5 µM 6-cyano-7-nitroquinoxaline-2,3-dione (CNQX), 10 µM D-2-amino-5-phosphonopentanoate (AP5, Alexis), and 10 µM bicuculline were added to the external solution. In pressure ejection experiments, tetrodotoxin (TTX, Alomone, 0.5 µM) was added to the bath to block synaptic transmission.

The electrode solution contained (in mM) 125 KCl, 1 $CaCl_2$, 10 1,2-bis(2-aminophenoxy)-ethane-*N*,*N*,*N*',*N*'-tetraacetic acid (BAPTA), 2 $MgCl_2$, 4 Na_2ATP, 10 *N*-2-hydroxyethylpiperazine-*N*'-2-ethanesulfonic acid (HEPES), pH adjusted to 7.2 with KOH. In our experiments, the calculated equilibrium potential for Cl^- was +1.0 mV. Therefore, with the holding potential of –70 mV, we observed IPSCs as inward currents. When e-IPSCs were tested, 5-lidocaine-*N*-ethyl bromide (QX-314, RBI, 5 mM) was added to the electrode solution to intracellularly block fast sodium currents [5]. In order to reduce glycine uptake, NaCl in the external solution was replaced by choline chloride (ChCl) assuming that the uptake of glycine is sodium dependent [17, 26]. We also used the specific blocker of the glycine transporter GLYT1 [21], sarcosine. For intracellular acidification, 30 mM of the external NaCl was replaced by an organic weak acid salt, sodium propionate [33], and pH was adjusted to 7.4.

Octanol (1-octanol, Sigma) was dissolved in dimethyl sulphoxide (DMSO) at a concentration of 1.5 M and stored at –20°C. The final concentration of DMSO in the external solution did not exceed 0.05 vol% (3.2 mM). At a concentration of 0.05 vol%, DMSO itself did not change the amplitudes or the decay kinetics of e-IPSCs (n=3) and directly evoked glycinergic currents (n=3, data not shown). Drugs were purchased from Sigma (St. Louis, Mo., USA) unless indicated.

Protocol

Hypoglossal motoneurons were voltage-clamped at a holding potential of –70 mV. IPSCs were evoked by electrical stimulation of either the ipsilateral or contralateral reticular formation, ventral and immediately outside of the hypoglossal nucleus [36] or the Nucleus of Roller which contains inhibitory neurons [3]. For stimulation, we used a bipolar platinum wire electrode (30 µm diameter; generous gift from DEGUSA, Germany, distance between two wires: 50 µm) custom-fabricated with a theta-style, two-channel borosilicate glass capillary (Clark Electromedical, Pangbourne, UK). The stimulus (9–90 V, 0.5 ms pulse duration, 0.1 Hz, 10 pulses) was adjusted to yield an IPSC of consistent amplitude >100 pA (range 180–1460 pA, n=37). For evoking glycinergic currents, glycine (100 mM) was applied from a glass pipette using a custom-made pressure ejection system with an electromagnetic valve controlled by the "Pulse" software. The glass pipette for pressure ejection had a resistance of 2 MΩ and was placed 20–50 µm above the recorded motoneuron. Glycine was applied every 30 s with a brief pressure pulse (20 ms, 10–220 kPa or 0.1–2.2 bar) throughout the experimental protocol. The current responses to a negative 10-mV voltage step (20 ms) from the holding potential of –70 mV were recorded after every ten stimuli or ten pressure ejections to monitor input resistance. We waited for 10 min after bath application of any drug to start new eIPSC or direct glycinergic current measurements.

Data analysis

Stimulus-evoked IPSCs and direct glycinergic currents were analyzed using IGOR Pro software (WaveMetrics, Oregon, USA). The peak amplitude was determined by averaging ten consecutive IPSCs. The time constant of the decay phase (τ_{decay}) was calculated by iterative single exponential curve fitting using the Levenberg–Marquardt algorithm. The curve fitting was applied to the

range where the current decreased below 90% of the maximum current. To determine the reversal potential of e-IPSCs, responses were measured at seven different holding potentials ranging between –70 mV and +50 mV, and fitted by linear regression with the least-squares method. In the analysis of direct glycine-evoked currents, the peak amplitude was determined by averaging three consecutive current responses. The time constant of decay was calculated using the fast component of the decay phase where the current decreased below one-half of the maximum current. Results are expressed as means ±SE. The paired *t*-test was used to determine the significance of changes. Differences were regarded as significant when $P<0.05$.

Results

Changes in e-IPSC kinetics

Stimulus-evoked currents were completely abolished by the application of strychnine (10 µM), suggesting that the responses were IPSCs due to activation of strychnine-sensitive glycine receptors (data not shown). As shown in Fig. 1A,B, octanol (1 mM) reduced e-IPSC amplitude by 78±9% ($n=5$, $P=0.03$), and prolonged the decay time constant by 202±67% ($n=5$, $P=0.009$). The effects were not due to failures. The variance of the time constant at a concentration of 1 mM octanol was large due to the decrease in signals associated with 78% reduction in IPSP amplitude (see Fig. 1B). After 10 min of wash, IPSC amplitudes recovered to 82±12% of control ($n=6$), whereas τ_{decay} remained increased by 61±12%. Longer wash periods were not attempted. Neuronal input resistance did not change even after application of 1 mM octanol ($n=9$, 138±30 MΩ versus 141±25 MΩ, $P=0.36$). The reversal potential for e-IPSCs did not change either after application of 500 µM octanol ($n=3$, 1.3±6.7 mV versus 2.6±4.9 mV).

Next we tested the dose-dependent effect of octanol on e-IPSCs. Octanol reduced amplitudes (Fig. 1C) and lengthened τ_{decay} (Fig. 1D) in a dose-dependent manner. The reduction of amplitudes became significant at the concentration of 250 µM (25±3%, $n=4$, $P=0.02$). The concentration at half-maximal effect (EC_{50}) on IPSC amplitude was estimated by fitting the equation (Eq. 1) to the mean IPSC amplitude at five different concentrations of octanol ($n\geq3$ at each concentration).

$$IPSC\ amplitude\ (\%control) = \frac{100}{1+(EC_{50}/[octonol])^{n}}$$

where [octanol] is the octanol concentration and *n* is the slope factor of the response curve similar to the Hill coefficient. The iterative non-linear least-squares curve fit (Fig. 1C) resulted in an EC_{50} of 475 µM and a slope factor of –1.64. The effect of octanol on the time course of IPSC decay was evident at a concentration of 250 µM (37±5% increase, $n=4$, $P=0.02$, Fig. 1D).

Fig. 1A–D Octanol reduces the amplitude and prolongs the inhibitory postsynaptic current (*IPSC*) decay evoked by stimulating the ventral border of the hypoglossal nucleus. **A** Representative responses recorded from one hypoglossal neuron, showing that octanol reduces the amplitude of stimulus-evoked IPSCs (*e-IPSC*). Each *trace* is the average of ten consecutive responses (10-s interval). Stimulus artifacts are truncated. **B** e-IPSCs in **A** are normalized with respect to the peak amplitude of each response. Octanol remarkably prolongs decay phases of e-IPSCs. The signal-to-noise ratio of the response with 1 mM octanol is low, due to a large amount of decrease in the amplitude. Note that the decay phase is still prolonged after 10 min wash out. **C** Effects of octanol on e-IPSC amplitude are dose-dependent. Data points are shown as means (% of control) ±SD ($n>3$ for each concentration). The result of curve fitting according to Eq. 1 is also shown. **D** Effects of octanol on time constants of IPSC decay phases (τ_{decay}) increase exponentially with the increase in octanol concentration. Data points are shown as means (% of control) ±SE ($n>3$ for each concentration). $^{*}P<0.05$; $^{**}P<0.01$

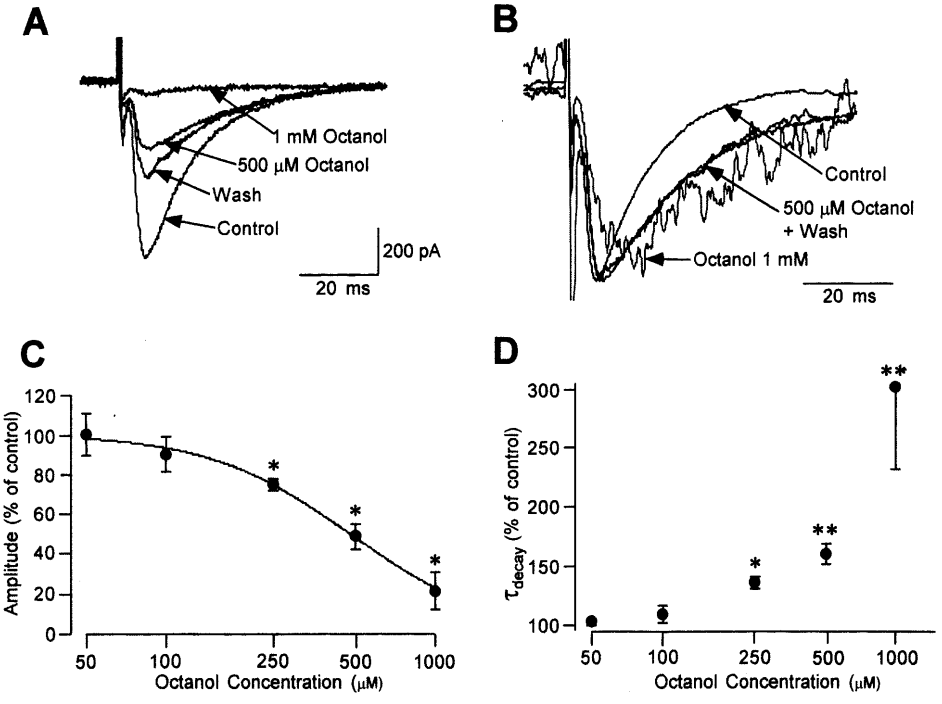

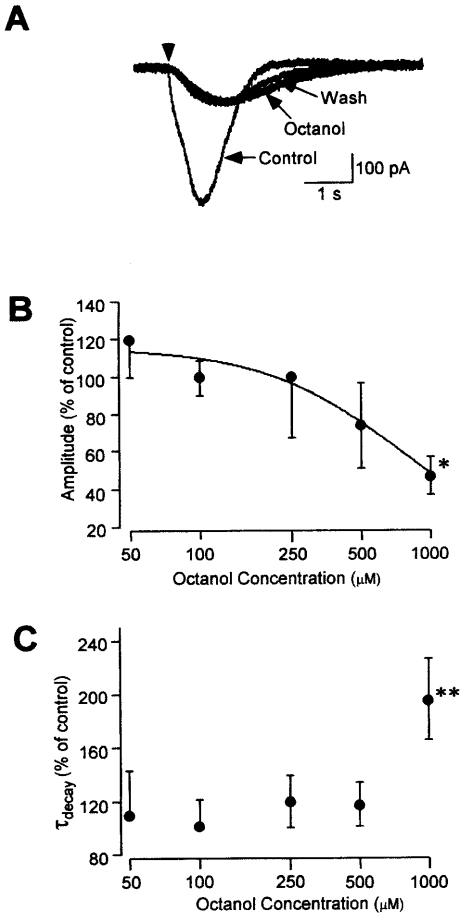

Fig. 2A–C Octanol decreases the amplitude and lengthens the time course of glycinergic currents (I_{gly}). Currents were evoked in the presence of tetrodotoxin (*TTX*, 0.5 μM) by local pressure ejection of 100 mM glycine above the soma of recorded hypoglossal neuron. **A** Octanol (1 mM) decreases the amplitude and prolongs the decay phase of I_{gly}. Each *trace* is the average of three consecutive I_{gly} responses (30-s interval). The timing of pressure ejection is marked as ▼. The decay phase is shortened but there is no recovery in the amplitude after 10 min of wash. **B** Dose-dependent effects of octanol on the peak amplitude of I_{gly}. **C** Dose-dependent effects of octanol on the peak amplitude of τ_{decay}. In **B** and **C**, data points are shown as means (% of control) ±SE (n>3 for each concentration). $^{*}P$<0.05; $^{**}P$<0.01

Changes in direct glycine-induced currents

The effect of octanol on glycine-evoked currents (I_{gly}) was tested in the presence of 0.5 μM TTX to examine the effects of octanol on membrane responses independent of any effects on transmitter release (Fig. 2). I_{gly} was evoked by direct pressure ejection of glycine to hypoglossal motoneurons (see Materials and methods). The currents were completely abolished by application of strychnine (10 μM), suggesting that the currents were generated through the opening of strychnine-sensitive ligand-gated Cl^- channels (data not shown). The dose-dependent effect of octanol on I_{gly} is shown in Fig. 2B, C. The reduction of amplitudes by octanol was dose-dependent (Fig. 2B). The iterative non-linear least-squares curve fit using Eq. 1 (Fig. 2B) resulted in an EC_{50} of 758 μM and a slope factor of –1.42. The prolongation of τ_{decay} was only evident at the concentration of 1 mM (Fig. 2C). Octanol (1 mM) reduced the peak I_{gly} by 54±10% (n=8, P=0.02) and prolonged τ_{decay} by 97±31% (641±203 ms versus 1078±253 ms, n=8, P=0.001). The resting neuronal input resistance increased by 17±5% (n=5, P=0.02) with application of octanol in these experiments.

Effect of uptake blockers on e-IPSCs and responses to exogenous glycine

It is possible that changes in IPSC decay kinetics were caused by an effect of octanol on the glycine uptake mechanism. To test this possibility, we evaluated the effects of glycine uptake blockade on e-IPSCs and I_{gly} (Fig. 3). Seventy-five to eighty percent replacement of extracellular Na^+ reduces [^{14}C]glycine uptake in rat spinal cord slices to 15–20% of normal [26], and 0 mM extracellular Na^+ decreases [^{3}H]glycine or [^{14}C]glycine uptake in pigeon brain homogenates to 7% of normal [17]. We examined the effect of 80% replacement of extracellular Na^+ by choline. Exchange of the extracellular solution was confirmed by an abrupt decrease in membrane potential [35]. Additionally, in some cells, a decrease in action potential height was observed in the current-clamp mode. These modifications usually stabilized within 10 min and data were taken 15 min after the replacement. Na^+ substitution reduced IPSC amplitude by 39±19%; however, the response was inconsistent and did not reach statistical significance (Fig. 3C, n=4, P=0.06). The onset of current responses was delayed by the application of choline, probably due to the reduction in the sodium current responsible for axonal signal conduction. There was also no change in τ_{decay} (Fig. 3A and C, 18.7±3.5 ms versus 19.8±3.8 ms). We further tested the effects of Na substitution on I_{gly} evoked by pressure-ejected exogenous glycine to evaluate the validity of using low Na^+ to block glycine uptake. As summarized in Fig. 3C, sodium substitution decreased the amplitude of I_{gly} by 35±2% (n=3, P=0.02) and lengthened τ_{decay} by 111±19% (305±16 646±74, n=3, P=0.02), suggesting that sodium substitution changed I_{gly} decay kinetics by reducing glycine uptake, possibly under the condition of excessive amounts of glycine. Sodium substitution also increased resting input resistance by 19±7% (n=6, P=0.04).

We then examined the effect of octanol on glycinergic currents in low Na^+ external solution. As exemplified in Fig. 3B, octanol (1 mM) prolonged τ_{decay} of I_{gly} by 57±22%, even after 80% of Na^+ was substituted with choline (n=3, P=0.04).

The effect of sarcosine (500 μM) on e-IPSCs and I_{gly} was tested (Fig. 4). Sarcosine is a glycine transport inhibitor that is specific against glycine transporter subtypes GLYT1a and GLYT1b, but ineffective against GLYT2 [21]. In order to examine whether GLYT1 was

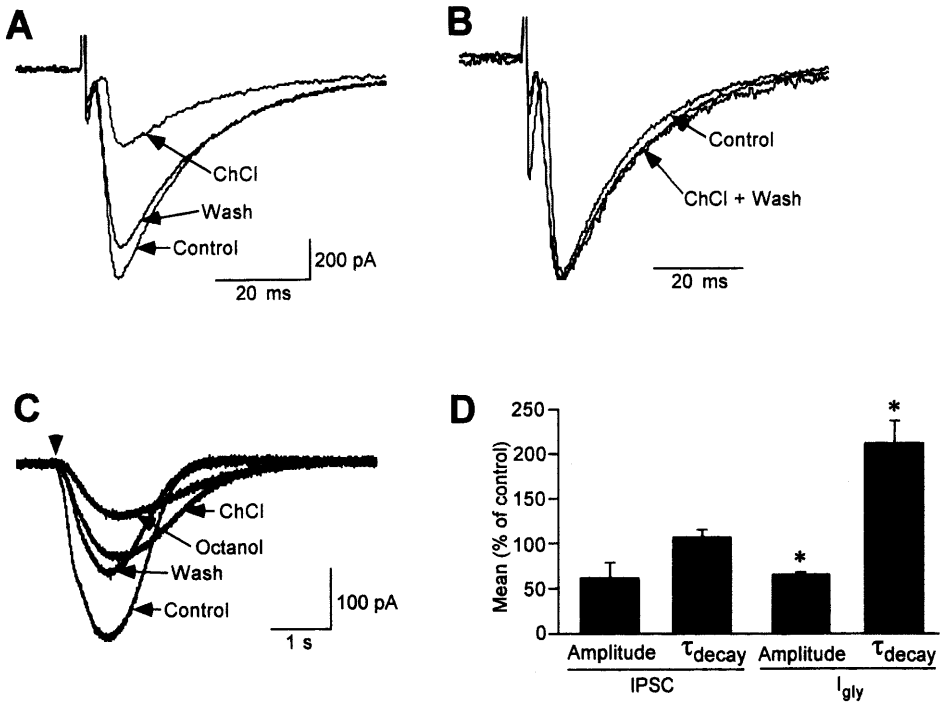

Fig. 3A–D Changes in e-IPSCs and glycinergic currents by 80% Na^+ substitution with choline (*ChCl*). **A** Representative e-IPSCs responses in one hypoglossal neuron, normalized with respect to the peak amplitude of each response. ChCl does not alter the decay kinetics of e-IPSCs. Note that the latency of the current responses was increased by Na^+ substitution. **B** ChCl decreases the amplitude and prolongs the decay phase of I_{gly} evoked by pressure ejection of glycine (100 mM). Octanol (1 mM) further reduces the amplitude and prolongs the decay phase. Representative responses recorded from a single hypoglossal neuron. Each *trace* is the average of three consecutive I_{gly} responses (30-s interval). **C** Mean changes in peak amplitude and τ_{decay} of e-IPSCs (n=4) and I_{gly} (n=3) by ChCl as a percentage of control. *Error bars* represent SE. $^*P<0.05$

present in our preparation, we tested the effect of sarcosine on I_{gly} (Fig. 4C, D). Sarcosine prolonged the decay phases of glycinergic currents by 103±11% (416±38 ms versus 841±69 ms, n=3, P=0.006), indicating that sarcosine changes the decay kinetics of glycinergic currents by blocking the existing GLYT1 glycine transporter. Changes in amplitude of I_{gly} were variable. In two of three cells, I_{gly} increased and in the other I_{gly} decreased. As illustrated in Fig. 4A,B, sarcosine did not change IPSC amplitude (727±198 pA versus 720±275 pA) or τ_{decay} (18.6±3.2 ms versus 17.5±3.2 ms) of e-IPSCs (n=4).

Effect of intracellular acidification by sodium propionate

Pappas et al. [28] have shown that octanol causes rapid initial intracellular acidification. To elucidate whether the observed alterations in IPSC kinetics by octanol are indirect effects of intracellular acidification, we tested the effect of intracellular acidification on glycinergic currents (Fig. 5). Intracellular acidification was introduced by administration of a weak organic acid salt, sodium propionate (30 mM), to the ACSF [30]. Figure 5A,B exemplifies the changes in e-IPSCs. Intracellular acidification reduced the amplitude of e-IPSCs and produced a small but consistent prolongation of decay phases. Figure 5D summarizes the effects of intracellular acidification on amplitudes and τ_{decay}. Intracellular acidification resulted in a decrease in IPSC amplitude by 22±9% (Fig. 5A, n=6, P=0.03) and an increase in τ_{decay} by 18±6% (n=6, P=0.01). Neuronal input resistance was increased by 14±6% (n=12, P=0.04). The calculated equilibrium potential for Cl^- shifted in the positive direction by 7.9 mV due to the decrease in extracellular Cl^- concentration. Accordingly, the measured reversal potential for e-IPSCs increased by 11.5±8.0 mV (n=3, P=0.14), although it did not reach statistical significance. The effects of intracellular acidification on amplitudes as well as τ_{decay} of IPSCs were persistent even after 10 min of wash.

The influence of intracellular acidification was also tested on I_{gly} (Fig. 5C). Intracellular acidification significantly prolonged τ_{decay} of I_{gly} by 28±11% (n=6, P=0.04). The peak amplitude of I_{gly} was decreased by 27±13%; however, the effect was variable and did not reach statistical significance (n=6, P=0.10).

Comparison of the change in decay kinetics by glycinergic-current-potentiating drugs

We further tested whether the slowing of eIPSC decay time is a common feature of the drugs that potentiate glycine-induced Cl^- conductances and/or block gap junction function. Ethanol is another alcohol that is known to enhance glycine receptor function [24]. Halothane, a volatile anesthetic agent, also potentiates glycine-induced Cl^- conductances [24]. Similar to octanol, halothane blocks gap junction communication [29]. Figure 6 shows the comparison between the effects of octanol (1 mM), sodium propionate (30 mM), ethanol (40 mM) and halothane (2–4 mM) on τ_{decay} of e-IPSCs. Ethanol (40 mM) did not change τ_{decay} (n=4, 17.7±3.7 ms versus 17.7±3.5 ms), whereas halothane (2–4 mM) prolonged τ_{decay} by 14±2% (25.0±8.1 ms versus 28.6±8.0 ms, n=4, P=0.03). The degree of the τ_{decay}-prolonging effect of halothane was comparable to that of sodium propionate, i.e., 18±6%, and was much less than that of 1 mM octanol.

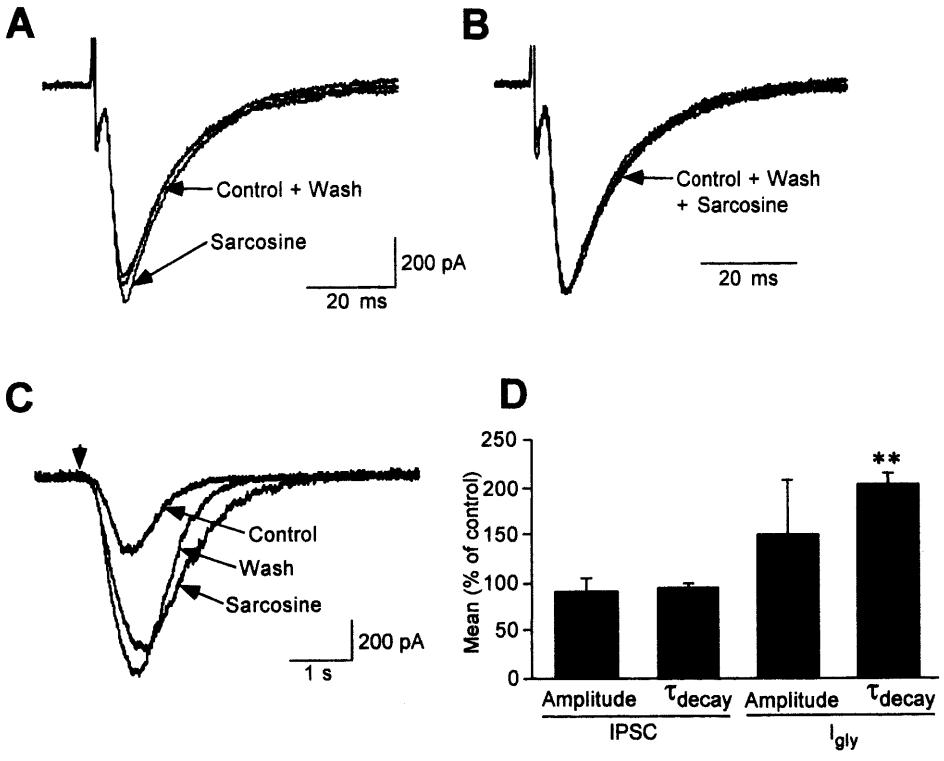

Fig. 4A–D Alterations in the amplitude and time course of e-IPSCs and glycinergic currents by sarcosine. **A** Representative responses recorded from one hypoglossal neuron, showing that sarcosine (500 µM) does not alter the amplitude of e-IPSC. Each *trace* is the average of ten consecutive responses (10-s interval). **B** e-IPSCs in **A** have been normalized with respect to the peak amplitude of each response. Sarcosine does not alter the decay kinetics of e-IPSCs. **C** Sarcosine (500 µM) prolongs the decay phase of I_{gly} evoked by pressure ejection of glycine (100 mM). In two of three cells, sarcosine enhanced the amplitude of I_{gly}. Representative responses recorded from a single hypoglossal neuron. Each trace is the average of three consecutive I_{gly} responses (30-s interval). **D** Mean changes in peak amplitude and τ_{decay} of e-IPSCs (n=4) and I_{gly} (n=3) by sarcosine as a percentage of control. *Error bars* represent SE. $^{**}P<0.01$

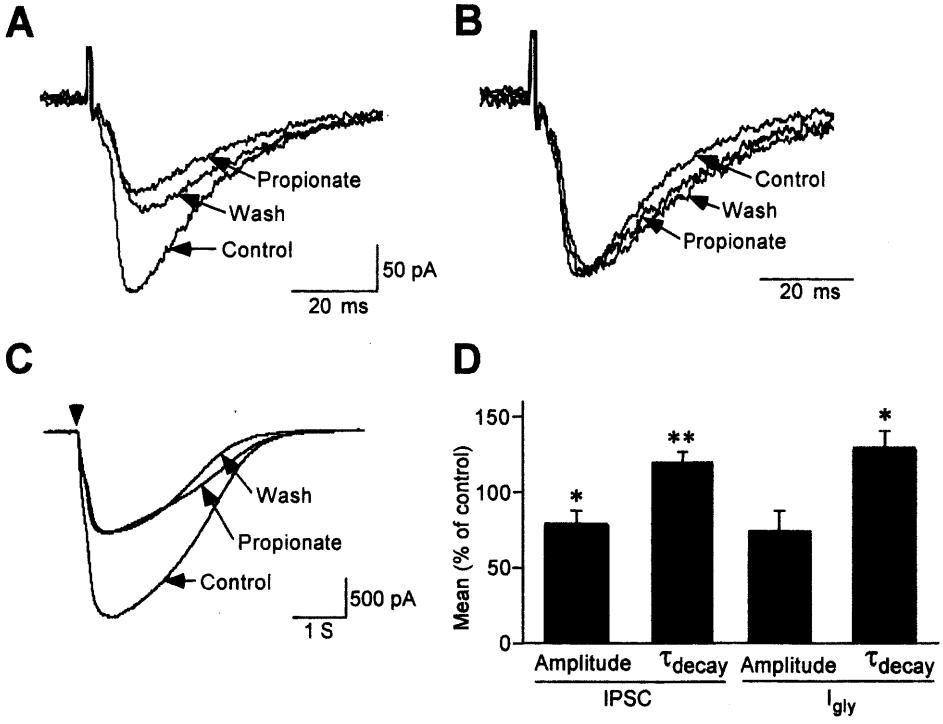

Fig. 5A–D Alterations in the amplitude and time course of e-IPSCs and glycinergic currents by intracellular acidification. Sodium propionate (30 mM) was used for intracellular acidification. **A** Representative responses recorded from one hypoglossal neuron, showing that propionate reduces the amplitude of e-IPSC. Note that little recovery has occurred after 10 min of wash. Each *trace* is the average of ten consecutive responses (10-s interval). **B** e-IPSCs in **A** have been normalized with respect to the peak amplitude of each response. Propionate prolongs the time course of IPSC decay phases by 18%. The prolongation persists after 10 min of wash. **C** An example of I_{gly} responses recorded from a single hypoglossal neuron. The responses were variant from cell to cell. Changes in amplitude ranges –51% to +5% and changes in τ_{decay} ranges –3% to +39%. **D** Mean changes in peak amplitude and τ_{decay} of e-IPSCs (n=6) and I_{gly} (n=6) by propionate as a percentage of control. *Error bars* represent SE. $^{*}P<0.05$; $^{**}P<0.01$

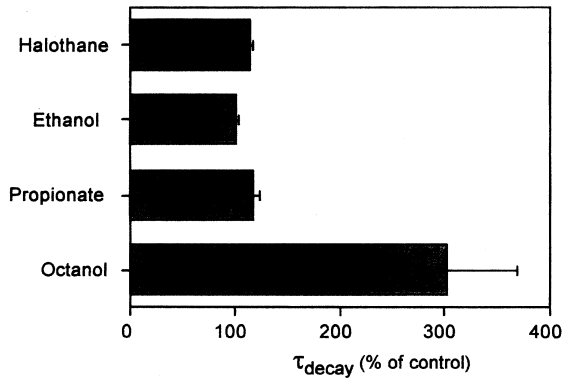

Fig. 6 Comparisons between the effects of octanol (1 mM), intracellular acidification by propionate (30 mM), ethanol (40 mM), and halothane (4 mM) on the time constant of eIPSCs

Discussion

The present study describes the effects of octanol on the kinetics of glycinergic IPSCs. We found that octanol produced a remarkable prolongation of IPSC decay time constant and a reduction of IPSC amplitude.

Changes in amplitudes of IPSCs and glycinergic currents

The reduction in glycinergic currents we observed in mouse brain slices is in contrast to the report of Mascia et al. [24], in which they described an enhancement of glycine currents in *Xenopus* oocytes. The discrepancy between the result of Mascia et al. [24] and ours could result from the difference in the composition of recepter subtypes, i.e., the difference between homomeric and heteromeric receptors. In their experiment, homomeric α2/α1 glycine receptor subunits were expressed in *Xenopus* oocytes, whereas the strychnine-sensitive glycine receptor consists of α2/α1 and β subunits that assemble in a pentameric structure with a proposed stoichiometry of 3α and 2β [4, 7]. This possibility is, however, quite speculative and single-channel outside-out recording is needed to determine whether beta subunits are responsible for the inhibitory effect of octanol. Apart from the direct effect on glycine receptors, several mechanisms associated with gap junction closure and intracellular acidification must be considered.

In whole-cell mode, amplitudes of synaptic currents depend on total conductances associated with a population of channels and the electrochemical gradients of current carriers. In neonatal neurons, total conductances may be influenced by electrically coupled neighboring cells. Therefore, gap junction blockade may decrease synaptic currents by decreasing the total conductances involved in the response. Thus, there is a possibility that gap junction closure of postsynaptic neurons contributes to the reduction in IPSC amplitudes and glycinergic currents.

A rapid intracellular acidification by 0.19 pH units upon application of 1 mM octanol has been reported [28]. This value is about half of the acidic shift observed (0.4–0.5 pH units) following 30 mM sodium propionate application [33]. As our internal solution contained 10 mM HEPES, the effects of intracellular acidification of recorded cells by octanol or sodium propionate might be different. Nevertheless, changes in intracellular pH might contribute to the reduction in IPSC amplitude by decreasing a HCO_3^- current component, since glycine receptors are permeable to HCO_3^- [8]. An increase in the intracellular H^+ concentration might cause a decrease in the intracellular HCO_3^- concentration, and the HCO_3^- equilibrium potential might shift to more negative voltages. In our experiments, however, octanol (500 μM) did not change the reversal potential of e-IPSC. Furthermore, the change in reversal potential by 30 mM sodium propionate (11.5±8.0 mV) was even more positive than the calculated change in Cl^- equilibrium potential due to the reduction of extracellular Cl^- concentration (6.9 mV). Therefore, we think that changes in HCO_3^- equilibrium potential caused by either octanol or propionate play only a minor role in the reduction of IPSC amplitude.

Changes in decay kinetics

We found that reduction of glycine uptake by Na^+ substitution or an inhibitor of glycine transporters did not change the kinetics of e-IPSCs (Figs. 3 and 4). The amount of transmitter liberated by electrical stimulation might be insufficient to observe any effect of reducing glycine uptake; however, this suggests that glycine uptake does not limit the removal of glycine from synaptic clefts during such asynchronous activity. This is consistent with the report of Titmus et al. [35] in which they did not observe any kinetic changes in electrically evoked glycinergic synaptic conductance of the goldfish Mauthner cell. However, we did observe a prolongation of decay time constants of direct glycine-induced currents. We reasoned that the amount of glycine given in the ejection experiment was much greater than that released by the electrical stimulation, thus the reduction of glycine uptake was only effective on I_{gly}. The glycine uptake system of astrocytes and neurons may be important in shaping synchronized activities, such as respiratory rhythm. During such synchronized activities, reciprocal inhibitory neuronal circuits and long-lasting periods of inhibition are essential [14, 32].

In contrast to the result on glycine uptake blockade, octanol remarkably changed the kinetics of e-IPSCs. Such octanol-induced prolongation of the time course of IPSC decay seems to result from mechanisms different from glycine uptake blockade. Moreover, octanol (1 mM) prolonged the decay phase of I_{gly} after reducing glycine uptake by Na^+ substitution, supporting the idea that the mechanism of octanol modulation of kinetics does not depend on glycine uptake. Apart from uptake, diffusion could limit the removal of glycine from synaptic clefts. Intracellular acidification by octanol [28] may

lead to glial swelling [15] and thus a decrease in extracellular space. However, our preliminary result showed that the intrinsic optical signal remained either unchanged or even decreased by the bath application of 1 mM octanol, suggesting that there was no decrease in extracellular space [18]. Therefore, the prolongation of decay time constants is not attributable to the diffusion interference by cell swelling.

It is interesting that gap junction blockade by both sodium propionate and halothane caused a small but significant increase in the decay time constant. This suggests that gap junction blockade partly contributes to the prolongation of the decay kinetics. However, the degrees of τ_{decay} prolongation by sodium propionate and halothane were not comparable with the 202% increase by 1 mM octanol (Fig. 6B). Therefore, the decay time prolongation by octanol is not likely to be related to gap junction blockade or intracellular acidification. Taking all these factors into consideration, we propose that the mechanism of decay time prolongation by octanol is most probably the direct action on glycinergic receptors of postsynaptic hypoglossal neurons, leading to prolongation of ligand binding to Cl^- channels. The change in decay kinetics is in line with the reported potentiation of glycine-induced Cl^- conductances by octanol, shown on glycine receptors expressed in *Xenopus* oocytes [24].

In conclusion, our data show that octanol has at least two distinct effects on glycinergic synaptic transmission, i.e., the prolongation of decay kinetics and the reduction of amplitude. These effects should be taken into account when one uses this drug as a gap junction blocker or a low-threshold calcium conductance blocker. Further studies are required to clarify the effects of long-chain alcohols as well as anesthetics on synaptic transmission.

Acknowledgements Yoshitaka Oku was supported by Alexander von Humboldt Foundation Research Fellowship. We thank Mirjam Haller and Dr. Sergeij Mironov for the measurement of the intrinsic optical signal, and Dr. P.M. Lalley for comments on the manuscript.

References

1. Aguayo LG, Pancetti FC (1994) Ethanol modulation of the γ-aminobutyric $acid_A$- and glycine-activated Cl^- currents in cultured mouse neurons. J Pharmacol Exp Ther 270:61–69
2. Aguayo LG, Tapia JC, Pancetti FC (1996) Potentiation of the glycine-activated Cl^- current by ethanol in cultured mouse spinal neurons. J Pharmacol Exp Ther 279:1116–1122
3. Aldes LD, Chronister RB, Marco LA (1988) Distribution of glutamic acid decarboxylase and gamma-aminobutyric acid in the hypoglossal nucleus in the rat. J Physiol (Lond) 175: 100–112
4. Bechade C, Sur C, Triller A (1994) The inhibitory neuronal glycine receptor. BioEssays 16:735–744
5. Bellingham MC, Berger AJ (1996) Presynaptic depression of excitatory synaptic inputs to rat hypoglossal motoneurons by muscarinic M2 receptors. J Neurophysiol 76:3758–3770
6. Berger AJ, Bayliss DA, Viana F (1996) Development of hypoglossal motoneurons. J Appl Physiol 81:1039–48
7. Betz H (1991) Glycine receptors: heterogeneous and widespread in the mammalian brain. Trends Neurosci 14:458–461
8. Bormann J, Hamill OP, Sakmann B (1987) Mechanism of anion permeation through channels gated by glycine and γ-aminobutyric acid in mouse cultured spinal neurons. J Physiol (Lond) 385:243–286
9. Burt JM, Spray DC (1988) Single channel events and gating behavior of the cardiac gap junction channel. Proc Natl Acad Sci USA 85:3431–3434
10. Connors BW, Benardo LS, Prince DA (1983) Coupling between neurons of the developing rat neocortex. J Neurosci 3: 773–782
11. Curtis DR, Johnston GAR (1974) Amino acid transmitters in the mammalian central nervous system. Ergeb Physiol Biol Chem Exp Pharmakol 69:97–188
12. Dildy–Mayfield JE, Mihic SJ, Liu Y, Deitrich RA, Harris RA (1996) Actions of long chain alcohols on $GABA_A$ and glutamate receptors: relation to in vivo effects. Br J Pharmacol 118:378–384
13. Draguhn A, Pfeiffer M, Heinemann U, Polder R (1997) A simple hardware model for the direct observation of voltage-clamp performance under realistic conditions. J Neurosci Methods 78:105–13
14. Ezure K (1990) Synaptic connections between medullary respiratory neurons and considerations on the genesis of respiratory rhythm. Prog Neurobiol 35:429–450
15. Hansson E, Ronnback A (1995) Astrocytes in glutamate transmission. FASEB J 9:343–350
16. Harris RA, Mihic SJ, Dildy-Mayfield JE, Machu TK (1995) Actions of anesthetics on ligand–gated ion channels: role of receptor subunit composition. FASEB J 9:1454–1462
17. Henke H, Cuénod M (1978) Uptake of L-alanine, glycine and L-serine in the pigeon central nervous system. Brain Res 152: 105–119
18. Holthoff K, Witte OW (1996) Intrinsic optical signals in rat neocortical slices measured with near-infrared dark-field microscopy reveal changes in extracellular space. J Neurosci 16:2740–2749
19. Johnston MF, Simon SA, Ramon F (1980) Interaction of anaesthetics with electrical synapses. Nature 286:498–500
20. Kandler K, Douglas SB, Katz LC (1994) Neuronal dye-coupling and spontaneous activity are inversely related in developing ferret visual cortex. Soc Neurosc Abstr 20:215
21. Liu Q-R, López-Corcuera B, Mandiyan S, Nelson H, Nelson N (1993) Cloning and expression of a spinal cord- and brain-specific glycine transporter with novel structural features. J Biol Chem 268:22802–22808
22. Llinás RR (1988) The intrinsic electrophysiological properties of mammalian neurons: insights into central nervous system function. Science 242:1654–1664
23. Lo Turco JJ, Kriegstein AR (1991) Clusters of coupled neuroblasts in embryonic cortex. Science 252:563–566
24. Mascia MP, Machu TK, Harris RA (1996) Enhancement of homomeric glycine receptor function by long-chain alcohols and anaesthetics. Br J Pharmacol 119:1331–1336
25. Mienville JM, Lange GD, Barker JL (1994) Reciprocal expression of cell–cell coupling and voltage-dependent Na current during embryogenesis of rat telencephalon. Dev Brain Res 77:89–95
26. Neal MJ (1971) The uptake of [^{14}C]glycine by slices of mammalian spinal cord. J Physiol (Lond) 215:103–117
27. Nedergaad M (1994) Direct signaling from astrocytes to neurons in cultures of mammalian brain cells. Science 263 :1768–1771
28. Pappas CA, Rioult MG, Ransom BR (1996) Octanol, a gap junction uncoupling agent, changes intracellular [H^+] in rat astrocytes. Glia 16:7–15
29. Peinado A, Yuste R, Katz LC (1993) Extensive dye coupling between rat neocortical neurons during the period of circuit formation. Neuron 10:103–114
30. Perez–Velaquez JL, Valiante TA, Carlen PL (1994) Modulation of gap junctional mechanisms during calcium-free induced field burst activity: a possible role for electronic coupling in epileptogenesis. J Neurosci 14:4308–4317

31. Rekling JC, Feldman JL (1997) Bidirectional electrical coupling between inspiratory neurons in the newborn mouse nucleus ambiguus. J Neurophysiol 78:3508–3510
32. Richter DW, Ballantyne D, Remmers JE (1986) How is the respiratory rhythm generated? A model. News Physiol Sci 1:109–112
33. Rörig B, Klausa G, Sutor B (1996) Intracellular acidification reduced gap junction coupling between immature rat neocortical pyramidal neurones. J Physiol (Lond) 490:31–40
34. Soltesz I, Lightowler S, Leresche N, Jassik-Gerschenfeld D, Pollard CE, Crunelli V (1991) Two inward currents and the transformation of low-frequency oscillations of rat and cat thalamocortical cells. J Physiol (Lond) 441:175–197
35. Titmus MJ, Korn H, Faber S (1996) Diffusion, not uptake, limits glycine concentration in the synaptic cleft. J Neurophysiol 75:1738–1752
36. Umemiya M, Berger AJ (1995) Presynaptic inhibition by serotonin of glycinergic synaptic currents in the rat brain stem. J Neurophysiol 73:1192–1200